The Regulation of Galaxy Growth along the Size-Mass Relation by Star Formation, as Traced by Hα in KMOS3D Galaxies at $0.7 \lesssim z \lesssim 2.7$

Wilman+ 2020
ApJ, 891, 1
arXiv: 2002.09499

Presenter: K. Kushibiki

Contents

Abstract

Half-light size measured by Hα emission for 281 star-forming galaxies

- Ha-size = 1.19(median) x (stellar-continuum-size) with just ~43% scatter
- No residual trend with stellar mass, SFR, redshift, or morphology
- The only residual trend is with the excess obscuration of Hα by dust

Scatter in continuum size at a fixed M* ← scatter in halo spin parameters

→ Stability of the ratio of Hα size to continuum size demonstrates stability in

  - Halo spin
  - The transfer of angular momentum to the disk

→ Require local regulation by feedback process

Implication demonstrated by a toy model

- Upper limit on star-formation driven growth is sufficient to evolve *along* size-mass relation

→ Require other processes (preferential quenching of compact galaxies or mergers) to explain observed evolution of the size-mass relation of star-forming disk galaxies

1. Introduction
Structure of Galaxies

Disk

- Stable, rotationally supported structure
- Described by a declining exponential function
- Not only in the stellar component, but also in the gas
- Exist to high-z, at least z~3 (Turner+2017),
  dominant among high-mass population by z~2.2 (Wisnioski+2015),
  common in the most compact and passively evolving old galaxies (many references)

Bulge

- Dispersion dominated
- Formed by violent star formation at the center or by merger events

1. Introduction
Relation of components

In local universe …

- Star-formation surface density and molecular gas surface density (Bigiel+2008)
- Local density of star-formation and that of stars (González Delgado+2016)
- Size of star-forming disk ~ size of stellar disk (Fossati+2013)

Kinematically …,

- Mean specific angular momentum of disk ~ that of their halo (Burkert+2016)
- Distribution of angular momentum in typical galaxy disk is in narrower range than expected from accreted halo gas (e.g. Dutton+2009)
  - High angular momentum material exist at large radii and can't form new stars
  - Low angular momentum material can be removed by energetic SNe-driven winds

In high redshift …,

- Main Sequence ($0 < z < 3$) and Resolved Main Sequence (to at least z~1; Wuyts+2013)
- Half-light size in the Hα emission ≳ size in continuum light
  (Nelson+2012; individual highly SFGs, Nelson+2016a; stacked average for normally SFGs)
- Molecular gas disk size is also similar to the stellar and star-forming disks (Tacconi+2013)
  (In the highly SFGs, compact dust emission and extended CO emission; Calistro Rivera+2018)

1. Introduction
Aim of this paper

In this paper …

- Use KMOS^{3D} data to map Hα and measure Hα disk sizes in individual SFG
  → Whether the stacked result of Nelson+2016a apply for individual galaxies
  Whether size growth via star-formation is correlated with the stellar mass and SFR, etc.

Strength of KMOS^{3D} data compared to previous studies

- Deeper integration
- Spectral resolution enough to resolve Hα+[NII] emission line complex
- Hα emission over a larger redshift range

Key question: How galaxies grow in size through star-formation ?

2. The KMOS^{3D} Survey

KMOS^{3D}

- Hα+[NII] emission line complex in galaxies at $0.7 < z < 2.7$
- 24 IFUs with 2.8″ x 2.8″
- Targets were selected from 3D-HST and CANDELS (COSMOS, GOODS-S, UDS)
- Selection with Ks-mag < 23 and known spec/grism-z
- ~ 3- 30 hours integration for each galaxy

In this work ...

- 645 galaxies taken up until April 2017
- PSF minor axis FWHM: 0.3″ – 0.92″, median of 0.456″
- SFR used in this paper are computed from IR, UV and optical observations (Wuyts+2011)

3. Data Reduction

3.1. Basic Reduction

Identical to Wisnioski+2019 using SPARK code

Exception: Background subtraction & astrometry

- Bad pixel mask
- Flattening at the detector level
- Reconstruction of data cubes
  including a wavelength calibration with sky lines and a heliocentric correction
- Correction for the spatial illumination uniformity
- Flux calibration with standard star observation
- Sky lines subtraction using an adjacent sky frame

Essential to subtract a residual background level per frame due to significant variation in instrumental, sky and thermal background between object & sky

→ A factor of 3 reduction in continuum S/N in final co-adds

→ Derive and subtract a background value for each of the readout channels of the detectors
(Overestimate background value for bright sources)

3. Data Reduction

3.2. Astrometric Registration, Improved Background Subtraction and Generation of Combined Cubes

Preparation of cubes

- Partial combined cubes: Combined within a given observing setup
- Bootstrap cubes: Propagation of uncertainty

Obtain a flat background and astrometric shift

1. Make ① of Partial-cubes and ② (Fig. 1.)
2. Fitting ① to ② with parameters of …
    - Astrometric shift
    - Normalizing flux scale factor
    - Additive background correction per RO ch

→ median residual shift: 1.33 KMOS pix (~0.27″)

→ Total-combined cubes and Bootstrap cubes

Fitting Total-cubes to HST-image in order to correct absolute astrometry (the same procedure as above) (Some with a manual shift)

Fig. 1.

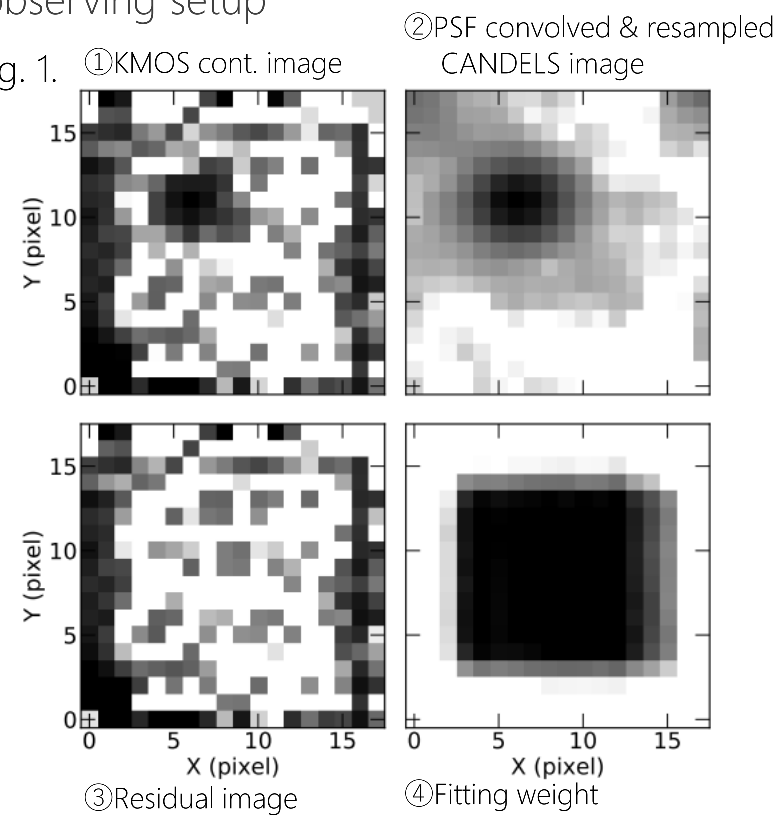

4. Generation of Maps and Profiles

IDL-based emission-line fitting software: KUBEVIZ (e.g. Fumagalli+2014, Fossati+2016)

4.1.1. Kinematic Fits

- Using flux, noise and bootstrap cubes *median smoothed* along spatial axes
- Assume continuum underlying Hα+[NII] as constant
  - Inverse-variance weighted average value around Hα

Continuum subtracted Data Continuum

$$\mathrm{CS_{x,y,\lambda} = F_{x,y,\lambda} - C_{x,y}}$$

- Fitting a single Gaussian; All lines share velocity and dispersion, Fixed [NII] ratio (3.071)

→ 2D map of line flux, velocity, dispersion

- Bootstrap cubes → Probability maps $\mathrm{P}_{\mathrm{f}_{\mathrm{H}\alpha}>0}$(detection significance),$\mathrm{P}_{\sigma>0}$ (resolution significance)

4.1.2. Masking

- ($f_{H\alpha}$ > 0) & (0 < σ < 250 km s^{-1})
  & ($\mathrm{P}_{\mathrm{f}_{\mathrm{H}\alpha}>0}$ ≥ 0.95) & ($\mathrm{P}_{\sigma>0}$ ≥ 0.9)
- 3σ clipping & remove isolated unmasked spaxels
- Smoothing with a 3x3 top-hat filter
- Remove galaxies with <3 valid spaxel & visual check
  → Leaving 455 galaxies

Fig. 2.

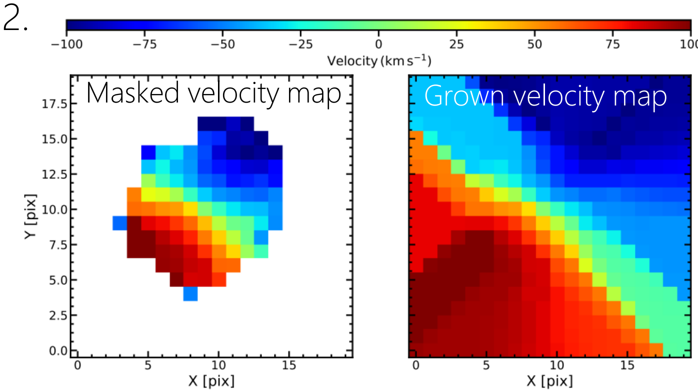

- Grown velocity maps $dv_{rest}(x,y)$ (average value of their neighbors)

4. Generation of Maps and Profiles

4.1.3. Deep emission line flux maps

- Using *unsmoothed* cube
- Narrow-band extraction: $\lambda_{cen}(x,y) = \lambda_{H\alpha}(1 + dv_{rest}(x,y)/c) \times (1+z)$

  with window width $\pm$200 km/s

→ $\mathrm{f_{H\alpha,WIN}(x,y) = \Delta\lambda \cdot \Sigma_{\lambda_{upper}(x,y)}^{\lambda_{lower}(x,y)} CS_{x,y,\lambda}}$

Correction for flux outside the narrow-band width

- Mask to define region with reliable velocity and dispersion
  → ($f_{H\alpha}$ > 0) & (0 < σ < σ_{max}) & ($P_{f_{H\alpha}>0} \geq 0.95$) & ($P_{\sigma>0} \geq 0.9$)
  σ_{max} = 1000 km/s ($S/N_{H\alpha}$>4), 400km/s ($S/N_{H\alpha}$<4)

→ With the dispersion measured by fitting, $\mathrm{f_{H\alpha,WINcor}(x,y) = f_{H\alpha,WIN}(x,y)/c_{\sigma_{200}}}$

(For spaxel defined as "bad" in the mask, they don't have reliable data to make correction, but these region are outer, low surface brightness and low dispersion < 100 km/s)

→ Hα flux map or image

4. Generation of Maps and Profiles

4.2. Image Fitting in 2D

Image fitting code: IMFIT (Erwin2015)

Continuum with Sersic profile

- F160W and F125W HST-image
- Free params: centroid, ellipticity, PA, r_e, n_{sersic}, normalizing surface brightness

Hα flux image with a simple exponential profile

- Centroid, ellipticity and PA are fixed to the value of continuum
- Case which are not well modelled by the exponential disk are flagged (Sec. 5.1)
- Trying with Sersic profile, confirm the trend presented in Sec. 6. are unchanged within uncertainty (For a substantial number of samples, Sersic fits hit the fitting limit)

4.3. Major axis profile

Elliptical annuli aligned to the galaxy's best fit ellipticity and PA

Fig. 3.

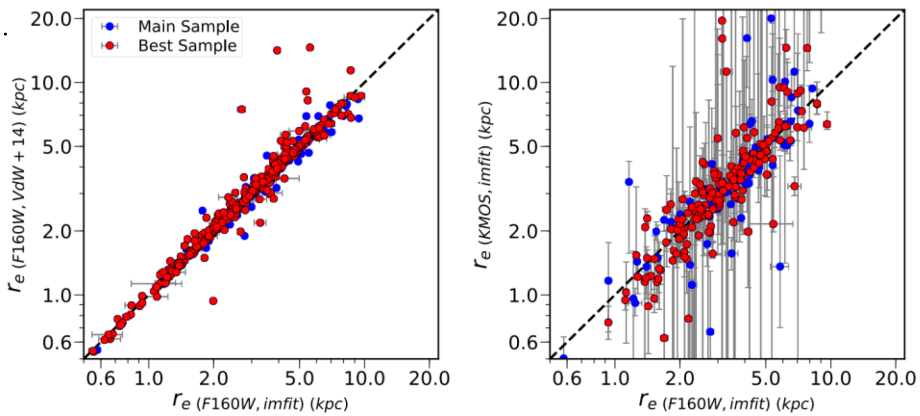

Fig. 4.

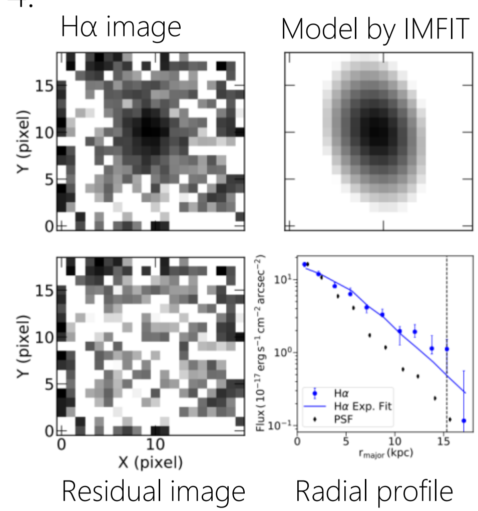

5. Sample

5.1. Flagging

Remove object with strong skyline contamination or poorly fit profiles (visual inspections)

- Atmospheric skyline residual contamination
  → 83/457 galaxies are removed, and 101 galaxies have weaker contamination (included)
- Close pair → 22 galaxies are removed
- Fitting accuracy → 399/457 meet criteria (207 excellent)
  1. Magnitude of fractional residual and $\chi 2$ value
  2. Agreement of extracted 1-D profile and best fit model
  3. IMFIT convergence
- CANDELS F160W ellipticities < 0.7 (i > 72.5)

→ 281 galaxies for MAIN samples, 89 galaxies for BEST samples (stricter than MAIN)

Not exclude 42 galaxies with broad lines (38 have known AGN)

5. Sample

5.2. Sample Bias

- High Hα detection fraction for MS galaxies
- Non-detections and Unmapped galaxies accounts for
  - 83% of UVJ passive galaxies
  - 98% of galaxies more than 1dex below MS
- Unmapped galaxies reach ~20% for $\log(M_*/M_\odot) > 10.9$ on MS

Fig. 5.

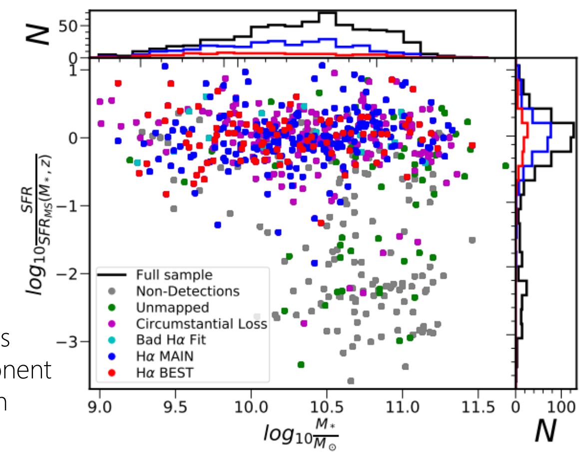

Unmapped: low-S/N or chaotic kinematics /dominant broad line component

Circumstantial Loss: Skyline contamination or high ellipticity

- Hα MAIN sample probes well into the dusty SF region in UVJ diagram
- (Hα MAIN covers wide range of each parameter and there is no sample bias caused by flagging)
- There is no notable difference between Hα MAIN and Hα BEST

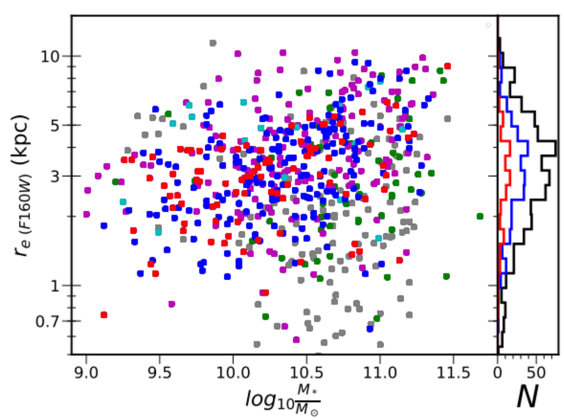

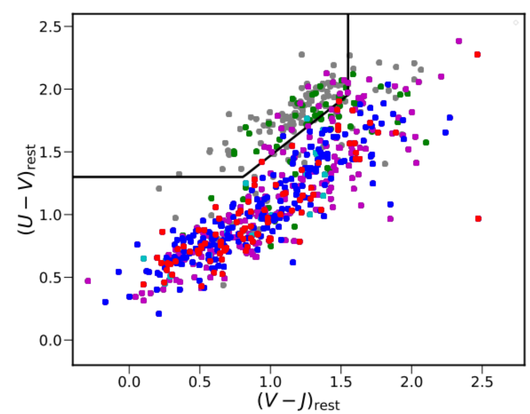

6. Results

6.1. Hα size correlations with continuum size and stellar mass

Best tracer for the size of old stars ← Size of SFGs is smaller at longer wavelength

- Rest-frame 6500AA sizes converted from the observed F160W sizes : $r_e(\mathrm{r6500})$
    - Close to the rest-frame wavelength probed by F160W
    - Close to the rest-frame wavelength of Hα

Fig. 6.

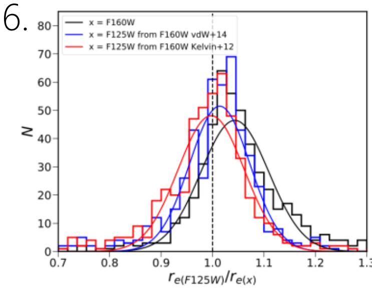

Whether Hα size of galaxies is better correlated with stellar size or total stellar mass ?

→ Both has correlation, but that with $r_e(\mathrm{r6500})$ is stronger and tighter

- Cont. size: slope=0.85 ± 0.05, σ=0.15dex(43%)
- Stellar mass: slope=0.18 ± 0.03, σ=68% (Roughly consistent with Nelson+2016a)

Importance of second parameter

→ Only continuum size is important

→ Star formation spatially tracks existing stars, but at a fixed continuum size global amount of stars has no relevance

Fig. 7.

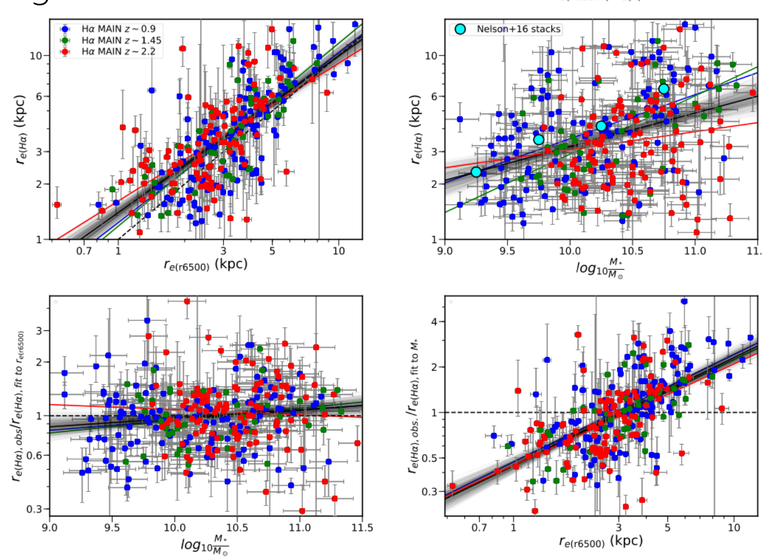

6. Results

6.1. cont'd

Difference of correlation between redshift range → No significant difference
(Slope = YJ: 0.93 ± 0.08, H: 1.00 ± 0.11, K: 0.75 ± 0.09)

Hα size at a particular continuum size

At median continuum size of 3.32 kpc
→ [Hα size] = 1.18(median),1.26(mean) x [cont. size]
(YJ: 1.13 ± 0.05, H: 1.17 ± 0.06, K: 1.20 ± 0.05
in median?)

Fig. 8.

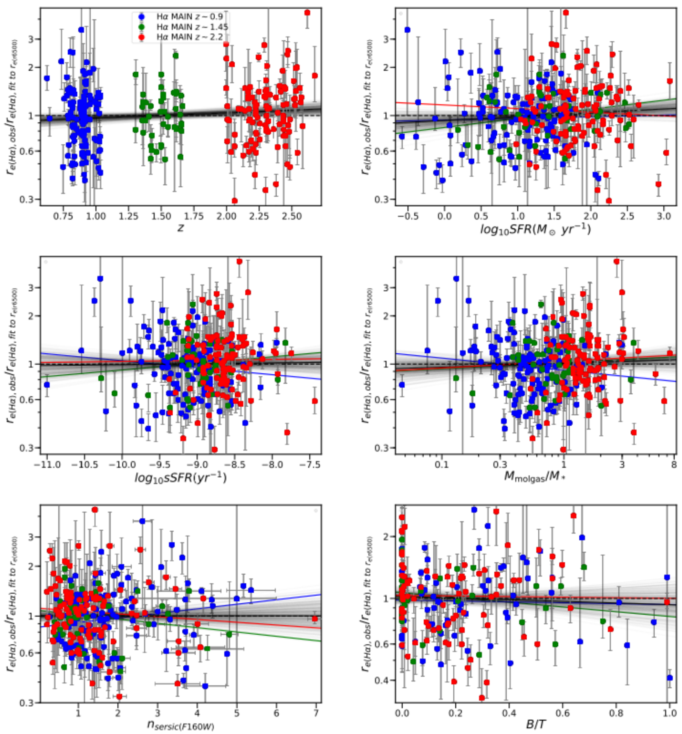

6.2. Which other parameters influence Hα size ?

Star formation activity, Morphology
→ No significant trend
nor any notable decrease in scatter

Key points here especially for morphology

- Contrast with the situation in the local Universe
  - SFG without bulge: Hα size ~ Cont. size
  - SFG with bulge: Hα size > Cont. size

In this paper, we can see the table testing more parameters (Table 1)

6. Results

6.3. Caveats

For Hα size,

- More diffuse component and additional sources of ionization
- Obscuration by dust, especially in dense and IR bright starburst region (Tadaki+2017)

For continuum size,

- Does continuum "emission" correctly trace the stellar mass in the galaxy?
  → Ratio of half-mass size to half light size $r_e(M_*)/r_e(\mathrm{r6500})$ decreases for high n_{sersic} mainly because of bulge with high mass-to-luminosity ratio
  → No correlation between $r_e(M_*)/r_e(\mathrm{r6500})$ and $r_e(H\alpha)/r_e(\mathrm{r6500})$
  → With continuum light, we are tracing "disk"

For dust extinction

- Extra extinction for Hα (Typically strong at the center)
  → Make observed Hα size larger than true size
  → The ratio of Hα to continuum size is an upper limit
  (Consider in detail in the next subsection)

Fig. 9.

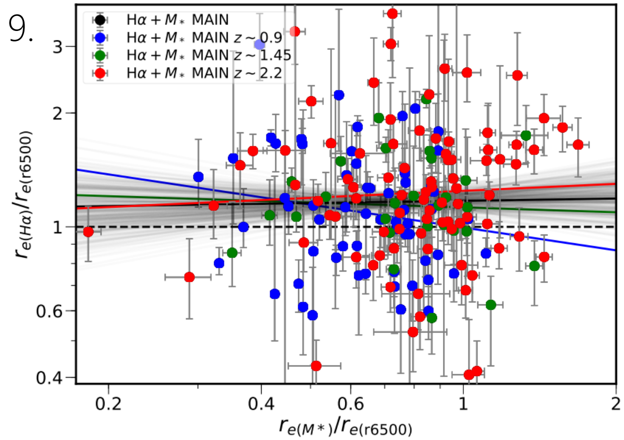

6. Results

6.4. Dependence on dust

SFR(from IR phot or SED)/$L_{H\alpha}$: Dust corrected conversion factor / Dust obscuration of Hα

$r_e(H\alpha)_{,obs}/r_e(H\alpha)_{,fit\ to\ r_e(\mathrm{r6500})}$ doesn't depend on Av, but has negative dependence on log(SFR/$L_{H\alpha}$)

→ $A_{H\alpha}$/Av decreases for galaxies with larger Hα size

This originate in the internal geometries of dust differently affecting young and old stars in galaxies

- Li+2019: The fraction in a foreground screen increase with galactic-centric radius and rest live in HII-region
  → Galaxies with large Hα disk are less subject to extra obscuration for Hα

Fig. 11.

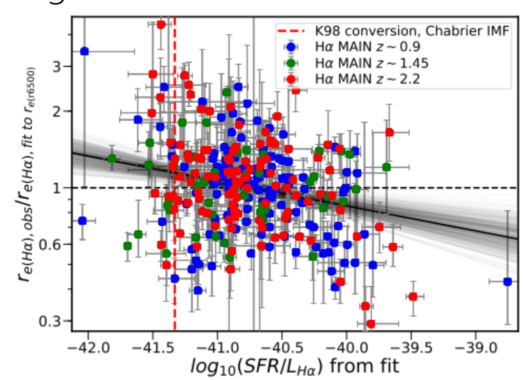

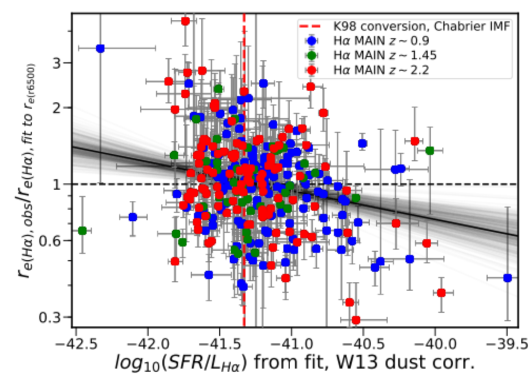

Fig. 10.

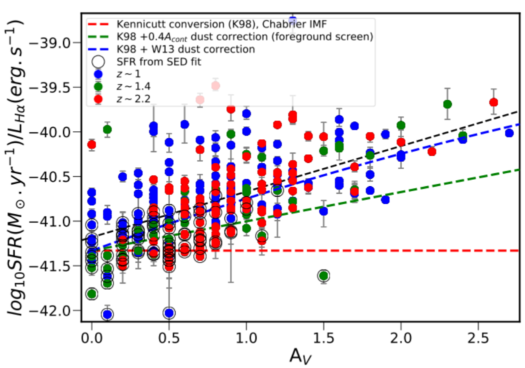

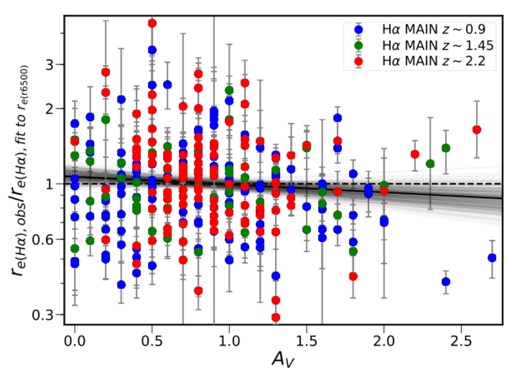

7. Interpretation

7.1. Analytic consideration

A simplified prediction for disk sizes: $R_d \propto H(z)^{-2/3} \cdot \lambda' \cdot M_{halo}^{1/3}$ (Mo, Mao & White 1998)

Galaxy spin parameter: $\lambda' = \lambda \cdot \frac{j_d}{m_d}$

(λ: halo spin parameter, j_d, m_d: a fraction of halo angular momentum, halo mass in the disk)

Applying this relation to the star-forming disk,

$$\frac{R_{d,SF}}{R_{d,*}} \propto \left(\frac{H(z_{SF})}{H(z_*)}\right)^{-2/3} \cdot \frac{\lambda'(z_{SF})}{\lambda'(z_*)} \cdot \left(\frac{M_{halo,z_{SF}}}{M_{halo,z_*}}\right)^{1/3}$$

With the observation result, strong correlation of Hα size with continuum size with small scatter

→ The stability over time of the spin parameter

Intrinsic scatter of 43%

= (short time variation of λ) + (efficiency of angular momentum transfer from halo to disk)

Expected ratio from this relation

$R = [H(z_*)/H(z_{SF})]^{2/3} = 1.33, 1.59$ for $(z_{SF} = z_{obs},\ z_*) = (1, 1.5), (2, 3)$

$P = \left[M_{halo,z_{SF}}/M_{halo,z_*}\right]^{1/3} = 0.8, 0.7$ (Fakhouri, Ma & Boylan-Kolchin 2010)

→ $R_{d,SF}/R_{d,*} \sim [1.11, 1.06] \cdot \lambda'(z_{SF})/\lambda'(z_*)$

→ Lack evolution mean that specific angular momentum of SF material is stable over many Gyrs

7. Interpretation

7.2. A toy model for evolution in size and mass

How star-formation in galaxies lead them to evolve in the size-mass plane?

Model

- MS relation (Whitaker+2014) + log-nomal scatter ~ 0.3dex (Noeske+2007)
- Mass loss from stars with FSPS code (Conroy, Gunn & White 2009)
- Size growth factor (SGF): $r_e(SF)/r_e(M_*)$=const.
- Exponential profile
- At each step newly formed stars are generated in exponential distribution

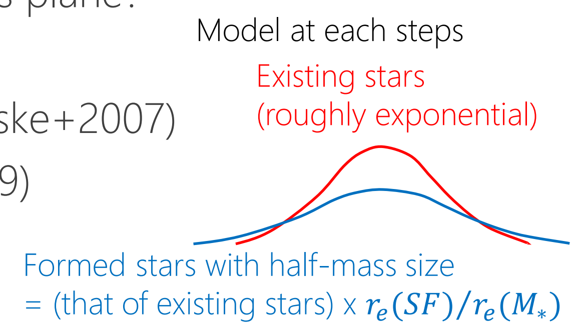

With different size growth factor …

Goal: Explain the evolution of size-mass relation
for late type galaxies from van der Wel+2014b

Fig. 12.

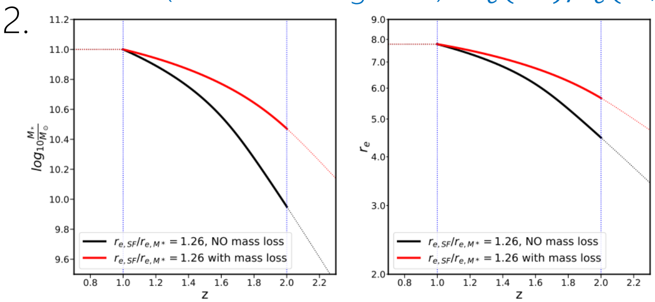

Fig. 13.

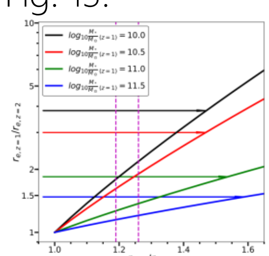

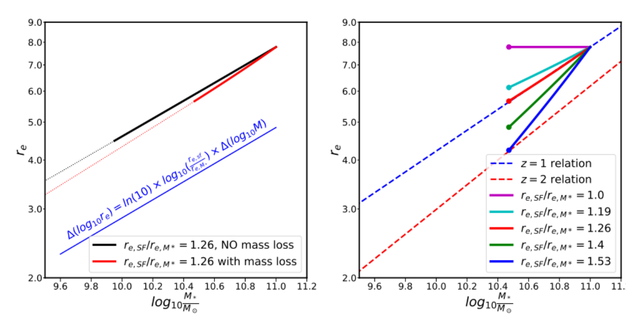

- $r_e(SF)/r_e(M_*)$=1.26 explain only evolution *along* the size-mass relation
- Large size growth factor is required $r_e(SF)/r_e(M_*)$~1.50-1.60

7. Interpretation

7.3. Considerations and constraints on evolution

Which previous result is the most suitable to be compared with the result of this paper?

1. van der Wel+2014 find evolution ($\sim H(z)^{-2/3}$) and stellar mass dependence ($M_*^{0.22}$) in *half-light size*
   ↔ Suess+2019 find little dependence on stellar mass or redshift in *half-mass size*
2. Without star formation driven size growth, there would be no age-gradient.
   ↔ Larger size at shorter wavelength. The result of this paper ($r_{H\alpha}/r_{cont}=1.26$)
3. Constant size growth factor $r_e(SF)/r_e(M_*)$ keep age gradient
   ↔ The lack of M/L gradient at z=2 seen by Suess+2019
   We find the difference mass vs light sizes due to the difference of bulge contribution.
4. No correlation of $r_e(H\alpha)/r_e(\mathrm{r6500})$ and $r_e(M_*)/r_e(\mathrm{r6500})$
   → The difference of main driver of variation, dust attenuation and bulge contribution
   → Continuum light and Hα are more closely tied than mass and Hα.

→ Compare to the simpler, light-based van der Wel+2014 relation

→ Cannot match the observed evolution

→ Other physical processes for growth of star forming galaxies might be at play

7. Interpretation

7.4. Physical origins of galaxy size growth

If evolution of size-mass relation by van del Wel+2014 is real
→ Another form of growth not associated to star-formation
i.e.) The stellar component evolve in size due to angular momentum transfer with the surrounding material (gas and dark matter)

Feedback for regulation and shallow evolution

Constant size growth factor
→ Halo spin parameter and the specific angular momentum transfer is stable under varying condition
→ e.g.) Regulation via feedback

Result and modelling in this paper: $\frac{d\log(r_e)}{d\log(M_*)} \sim 0.26$

- consistent with the estimate from study of Milky-Way progenitor ($\frac{d\log(r_e)}{d\log(M_*)} \sim 0.27$)
- Shallower than van Dokkum+2015 (~0.3) and simulated galaxies with wind model of Hirschmann+2013 (~0.4)

Efficient removal of low angular momentum material at high redshift leads to much larger size and shallower evolution

7. Interpretation

7.4. cont'd

Quenching

Some of massive galaxies will be quenched by z~1

Theories for process of quenching and compactness of passive galaxies

- Galaxies with low spin parameters can become unstable and contract before quenching (Dekel & Burkert 2014)
- Galaxies reach a threshold stellar mass surface density etc. before quenching (van Dokkum+2015)
- Older galaxies with higher density and small sizes depart first from the MS (Abramson & Morishita 2019)

→ The distribution of size-mass plane is not inconsistent with such a scenario of $\frac{d\log(r_e)}{d\log(M_*)} = 0.5$

→ "Such a strong apparent evolution can happen
even if the evolution of individual galaxies is relatively weak,
so long as the densest galaxies fall out of the star-forming population first
and become passive."

→ More aggressive quenching is required